Hyperventilation following head injury: Effect on ischemic burden and cerebral oxidative metabolism*

Jonathan P. Coles, PhD; Tim D. Fryer, PhD; Martin R. Coleman, PhD; Peter Smielewski, PhD; Arun K. Gupta, FRCA; Pawan S. Minhas, FRCS; Franklin Aigbirhio, Dphil; Doris A. Chatfield, BSc; Guy B. Williams, PhD; Simon Boniface,† FRCP; T. Adrian Carpenter, PhD; John C. Clark, DSc; John D. Pickard, FRCS; David K. Menon, PhD

Objective: **To determine whether hyperventilation exacerbates cerebral ischemia and compromises oxygen metabolism ($CMRO_2$) following closed head injury.**

Design: **A prospective interventional study.**

Setting: **A specialist neurocritical care unit.**

Patients: **Ten healthy volunteers and 30 patients within 10 days of closed head injury.**

Interventions: **Subjects underwent oxygen-15 positron emission tomography imaging of cerebral blood flow, cerebral blood volume, $CMRO_2$, and oxygen extraction fraction. In patients, positron emission tomography studies, somatosensory evoked potentials, and jugular venous saturation (SjO_2) measurements were obtained at $Paco_2$ levels of 36 ± 3 and 29 ± 2 torr.**

Measurements and Main Results: **We estimated the volume of ischemic brain and examined the efficiency of coupling between oxygen delivery and utilization using the SD of the oxygen extraction fraction distribution. We correlated $CMRO_2$ to cerebral electrophysiology and examined the effects of hyperventilation on the amplitude of the cortical somatosensory evoked potential response. Patients showed higher ischemic brain volume than controls (17 ± 22 vs. 2 ± 3 mL; $p \leq .05$), with worse matching of oxygen delivery to demand ($p < .001$). Hyperventilation consistently reduced cerebral blood flow ($p < .001$) and resulted in increases in oxygen extraction fraction and ischemic brain volume (17 ± 22 vs. 88 ± 66 mL; $p < .0001$), which were undetected by SjO_2 monitoring. Mean $CMRO_2$ was slightly increased following hyperventilation, but responses were extremely variable, with 28% of patients demonstrating a decrease in $CMRO_2$ that exceeded 95% prediction intervals for zero change in one or more regions. $CMRO_2$ correlated with cerebral electrophysiology, and cortical somatosensory evoked potential amplitudes were significantly increased by hyperventilation.**

Conclusions: **The acute cerebral blood flow reduction and increase in $CMRO_2$ secondary to hyperventilation represent physiologic challenges to the traumatized brain. These challenges exhaust physiologic reserves in a proportion of brain regions in many subjects and compromise oxidative metabolism. Such ischemia is underestimated by common bedside monitoring tools and may represent a significant mechanism of avoidable neuronal injury following head trauma. (Crit Care Med 2007; 35:568–578)**

KEY WORDS: **ischemia; hyperventilation; positron emission tomography; trauma; head injury**

In health, reductions in $Paco_2$ result in cerebral vasoconstriction and a reduction in cerebral blood volume (CBV) (1). Consequently, hyperventilation has been used for controlling intracranial hypertension following traumatic brain injury (TBI) (2–4). Increasing evidence suggests the presence of early cerebral hypoperfusion (and possibly ischemia) following TBI (5–7), and there are concerns that hyperventilation-induced reductions in cerebral blood flow (CBF) may cause ischemia (2, 8–12) and affect outcome (13). Such concerns have led to recommendations regarding hyperventilation therapy in head injury (2). These advocate the avoidance of hyperventilation within the first 24 hrs of injury, when CBF is commonly reduced (5). However, they still consider hyperventilation an appropriate therapeutic option in patients with intracranial hypertension during the later phases of injury.

Recent publications have highlighted continuing debate (14–16) and centered on the difficulty of defining clear evidence of a critically ischemic brain at risk of neuronal injury. Ischemia is classically defined as a CBF below the threshold for neuronal electrical failure but above that for failure of energy metabolism and ion homeostasis (17). Studies of human stroke have used oxygen-15 positron emission tomography

†Deceased.

***See also p. 663.**

From The Division of Anaesthesia, University of Cambridge, Addenbrooke's Hospital, Cambridge, UK (JPC, AKG, DAC, DKM); The Wolfson Brain Imaging Centre, University of Cambridge, Addenbrooke's Hospital (JPC, TDF, MRC, PS, AKG, PSM, FAD, DAC, GBW, SB, TAC, JCC, JDP, DKM); Department of Clinical Neurophysiology, Addenbrooke's Hospital (MRC, SB); and Department of Neurosurgery, University of Cambridge, Addenbrooke's Hospital (PS, PSM, JDP).

Supported, in part, by the Medical Research Council, by a Technology Foresight Award from the UK Government, and by a Royal College of Anaesthetists/British Journal of Anaesthesia project grant. Dr. Coles was funded by Research Training Fellowships from the Addenbrooke's Charities and the Wellcome Foundation and by a Beverley and Raymond Sackler studentship award and is currently funded by an Academy of Medical Sciences/Health Foundation Clinician Scientist Fellowship. Mrs. Chatfield was supported by a grant from the Fund for Addenbrooke's. Dr. Coleman was supported by an MRC Studentship award.

The authors have not disclosed any potential conflicts of interest.

Address requests for reprints to: Jonathan P. Coles, Box 93, Addenbrooke's Hospital, Cambridge CB2 2QQ, UK. E-mail: jpc44@wbic.cam.ac.uk

DOI: 10.1097/01.CCM.0000254066.37187.88

(^{15}O PET) to demonstrate the physiologic pattern of events following acute ischemia. These show that tissue with reduced CBF, relatively preserved or normal cerebral oxygen metabolism ($CMRO_2$), but markedly raised oxygen extraction fraction (OEF) can be defined as exhibiting "misery perfusion" (18). The physiologic nature of such critically perfused tissue is dynamic, and ultimately its survival is dependent on both the severity and the duration of ischemia. This has led some investigators to produce predictive physiologic thresholds for tissue viability based on measurements of CBF, $CMRO_2$, and OEF in experimental ischemia and clinical stroke (19–21). In TBI, although it is possible to estimate physiologic thresholds below which tissue is almost certainly destined for irreversible morphologic abnormality, such thresholds cannot be used to predict the full extent of irreversible damage (22). A depressed level of consciousness, therapeutic sedation, and trauma-induced mitochondrial dysfunction (23) can reduce metabolic rate (and hence coupled perfusion) in the injured brain and reduce critical CBF thresholds for ischemia (24). Conversely, epileptiform activity, spreading depression, or hypermetabolism associated with excitotoxicity may increase $CMRO_2$ and make "normal" CBF levels inadequate. A clear definition of ischemia in situations where $CMRO_2$ is altered depends solely on the demonstration of compensatory increases in local OEF.

It is essential that we ensure that current therapies do no harm. Although hyperventilation is known to reduce CBF, there is no convincing evidence that it results in true ischemia (14, 15). Furthermore, it is important to determine the extent to which common bedside monitors, such as jugular bulb oximetry, miss focal ischemia and whether reliance on such monitors may mislead and potentially result in harm.

We have used ^{15}O PET to investigate whether acute hyperventilation has the potential to induce cerebral ischemia and neuronal damage following TBI. These data have been analyzed in conjunction with somatosensory evoked potentials (SEPs) to elucidate the possible physiologic mechanisms responsible.

MATERIALS AND METHODS

Subjects

PET studies were undertaken on ten healthy volunteers (eight male, two female) with a mean (range) age of 30 (18–60) yrs and 30 head-injured patients with a mean (range) age of 35 (16–70) yrs (Table 1) (25–27). Patients had a median (range) postresuscitation Glasgow Coma Scale score of 7 (3–12), but, when recruited to this study, all patients required sedation and/or ventilatory support for ICP elevation or reductions in Glasgow Coma Scale score to <8.

The experimental data that we present were acquired in three subsets:

1. To elucidate the relationship between $CMRO_2$ and cerebral electrophysiology, baseline PET data from 14 patients were correlated with baseline SEP.
2. We undertook PET studies before and after hyperventilation in 18 patients (two of whom were included in subset 1) to study the effects of hypocapnia on cerebral physiology.
3. We had planned to obtain posthyperventilation SEP data during the same session as PET studies, but the complexity of this protocol meant that we achieved this only in two of these subjects. The effects of hyperventilation on the cortical SEP amplitude were therefore studied in a further seven of these patients on a separate occasion within the first 10 days of injury.

Although it was intended that patients undergo several imaging sessions at different time points following injury, it was not possible to obtain complete data sets in all subjects. In fact, this was only achieved in two subjects due to patient instability, lack of scan time, and equipment failure. The data were therefore acquired in three subsets.

All volunteers provided informed consent for studies, and assent was obtained from the next of kin for all patient studies. All studies were approved by the Local Research Ethics Committee at Addenbrooke's Hospital, Cambridge, UK, and by the Administration of Radioactive Substances Advisory Committee of the United Kingdom.

Clinical Protocols

Patients were managed with protocol-driven therapy aimed at maintaining ICP <20 mm Hg and cerebral perfusion pressure >70 mm Hg, as previously described (28) (Appendix). Patients who received surgical intervention (CSF drainage or decompressive craniectomy) or second-tier medical therapies (barbiturate coma or moderate hypothermia at 33–35°C) before PET imaging are specified in Table 1.

For ICP monitoring, an intraparenchymal probe was used (Codman MicroSensors ICP Transducer, Codman & Shurtleff, Raynham, MA). A fiberoptic right jugular bulb catheter (Baxter) was inserted and its position confirmed radiologically. Samples of arterial and jugular venous blood were drawn for simultaneous measurement of arterial blood gases and jugular venous saturation (SjO_2). Using protocol-driven therapy (28), SjO_2 was continuously measured and attempts were made to maintain levels >50%.

Hyperventilation Intervention

Following acquisition of data in patients at a $Paco_2$ of approximately 35–40 torr (~5 kPa), minute ventilatory volume was increased to achieve a $Paco_2$ reduction to about 30 torr (4 kPa). If $Paco_2$ levels fell below 25 torr (3.3 kPa) or SjO_2 fell below 50%, the extent of hyperventilation was modulated. Following a 10-min period of stabilization, data collection was repeated. Although hemodynamic stability was ensured by titrating fluids and vasoactive agents, sedative infusions were left unchanged.

Positron Emission Tomography

PET studies were undertaken on a General Electric Advance scanner (GE Medical Systems, Milwaukee, WI). Steady-state emission data for $H_2{}^{15}O$ (two 5-min frames), $C^{15}O$ (single 5-min frame), and $^{15}O_2$ (two 5-min frames) were used to generate parametric maps of CBF, CBV, $CMRO_2$, and OEF as previously reported (29). Images were analyzed using custom-designed automated software (PETAN) (30–32).

Region of Interest Based Analysis. A region of interest (ROI) map specifying 15 ROIs was drawn within normalized (Talairach) space (33) on a reference magnetic resonance image (Fig. 1). Physiologic variables were expressed as an average within these mixed gray and white matter ROIs, while recognizing that the effect of tissue heterogeneity on ^{15}O PET models would result in falsely low CBF and $CMRO_2$ values (34–36).

Estimation of Ischemic Burden. We used OEF to assess the burden of ischemia to avoid the confounding effects of drug- and injury-induced metabolic suppression on CBF and $CMRO_2$. Although it is difficult to find data that identify critical increases in OEF levels that still allow survival in the setting of ischemia, we have previously discussed and validated a technique for patients with TBI (37, 38). We estimated an individualized critical OEF threshold (OEF_{crit}; which equated to a cerebral venous oxygen content of 3.5 mL/100 mL) for each subject as follows

$$OEF_{crit} = \frac{(CaO_2 - 3.5)}{CaO_2} \quad [1]$$

where,

$$CaO_2 = 1.34\mathrm{Hb.SaO_2} + 0.003\mathrm{PaO_2} \quad [2]$$

Table 1. Patient data

Age, Yrs	Gender	Injury	Marshall Category[a]	GCS	Extracranial Injuries	PET Session	PET Interval, Hrs	Surgery	Second-Tier Therapies	GOS
64	M	Fall	NEML	12	No. of ribs	Day 1, SEP	15			MD
						Day 3, SEP	61			
69	M	Fall	NEML	10	No. of ribs	Day 1, SEP	23			MD
40	M	RTA	NEML	3		Day 1, SEP	20			SD
						Day 5, SEP	116	EVD		
						Day 7, SEP	166		DC	
						Day 10, SEP	240			
70	M	Fall	EML	10		Day 1, SEP	21	Craniotomy (R SDH)		D
26	F	RTA	NEML	3	No. of femur	Day 5, SEP	103	ORIF femur	DC	SD
						Day 10, SEP	223		B	
45	M	Assault	NEML	6		Day 3, SEP	49	Craniectomy (L SDH)	DC	SD
						Day 7, SEP	146			
34	M	Fall	NEML	9		Day 3, SEP	85			GR
19	M	RTA	DI 2	5	No. of 5th–7th lumbar vertebra and ribs	Day 7, SEP	179			MD
18	M	Assault	NEML	7		Day 2, SEP	38	Craniectomy (R EDH)	DC	MD
16	F	RTA	NEML	4		Day 2, SEP	40			D
23	M	Fall	EML	5		Day 4, SEP	87	Craniectomy (L SDH)	DC	MD
29	M	RTA	EML	6	No. of ribs	Day 1, SEP	14	Craniectomy (L EDH), EVD	DC	MD
						Day 5, SEP	133			
40	F	Fall	EML	8		Day 2 HV, SEP	40	Craniectomy (L SDH)	DC	SD
18	M	RTA	NEML	12	No. of 12th thoracic vertebra	Day 3 HV, SEP	67			MD
45	M	RTA	NEML	10	No. of clavicle and mandible	Day 3 HV	64			SD
25	M	RTA	NEML	7	Lung, kidney and spleen contused. Facial 0.05	Day 3 HV	59			MD
49	F	RTA	NEML	8	No. of ribs, diaphragmatic hernia	Day 3 HV	59	Laparotomy & repair of diaphragmatic hernia		SD
26	F	RTA	EML	5	No. of clavicle	Day 2 HV	42	Craniectomy (L SDH)	DC	GR
41	M	Fall	DI 2	7		Day 6 HV	134			MD
46	M	RTA	NEML	4	No. of tibia and fibula	Day 4 HV	84			
58	M	RTA	EML	7		Day 2 HV	41	Craniectomy (R ICH)	DC	D
36	M	Fall	EML	12		Day 2 HV	45	Craniectomy (L EDH)	DC	MD
27	M	Fall	EML	8	No. of zygoma and wrist	Day 2 HV	39	Craniectomy (R EDH)	DC	GR
16	M	RTA	NEML	8	No. of 2nd lumbar vertebra	Day 5 HV	110			GR
26	M	RTA	DI 2	3		Day 2 HV	37		H	GR
51	F	RTA	DI 2	5	No. of radius and femur	Day 3 HV	67			SD
31	M	Fall	DI 3	10		Day 7 HV	155	EVD	H, B	MD
25	M	Fall	DI 2	12		Day 5 HV	108			GR
17	M	Assault	DI 2	6		Day 7 HV	160		B	D
20	F	RTA	DI 3	7	Femur, pelvis, tibia, fibula, and facial nos.	Day 3 HV	59	EVD		SD

GCS, Glasgow Coma Scale (Ref. 25); PET, positron emission tomography; GOS, Glasgow Outcome Score (Ref. 26); NEML, nonevacuated mass lesion; #, fracture; SEP, somatosensory evoked potential recordings taken; MD, moderate disability; RTA, road traffic accident; EVD, external ventricular drain; SD, severe disability; DC, decompressive craniectomy; SDH, subdural hematoma; R, right; D, death; ORIF; open reduction and internal fixation; B, barbiturate coma; L, left; GR, good recovery; DI, diffuse injury; EDH, extradural hematoma; HV, hyperventilation; R ICH, right intracerebral hemorrhage; H, moderate hypothermia (core temperature ≈34°C).

[a]Ref. 27.

CaO_2 is arterial oxygen content, Hb is the hemoglobin in g/100 mL, and Sao_2 is the fractional arterial oxygen saturation.

Application of these thresholds to frequency histograms of OEF images allowed us to calculate the volume of voxels with cerebral venous oxygen content values below this threshold and hence allowed estimation of the ischemic brain volume (IBV) (Fig. 1). We compared the IBV to data derived from jugular oximetry, using a traditional threshold value for SjO_2 (50%) (2, 39–41).

Perfusion-Utilization Matching. We examined the relationships between changes (Δ) in CBF, $CMRO_2$, and OEF with hyperventilation in order to understand the pathophysiologic derangements induced by trauma. The calculations used to derive CBF, OEF, and $CMRO_2$ using ^{15}O PET make use of common emission data. Consequently, mathematical coupling could confound any exploration of the relationship between these variables (29). To generate data sets that were independent of such effects, we took advantage of the fact that our $H_2{}^{15}O$ and $^{15}O_2$ emission data were collected in two separate frames and used independent $H_2{}^{15}O$ and $^{15}O_2$ emission and arterial data to calculate mathematically independent CBF, $CMRO_2$, and OEF parametric maps.

OEF values from the 15 ROI template described previously should be closely clustered in normal subjects, suggesting efficient matching of CBF to $CMRO_2$, with a resulting narrow spread of OEF values (42). We assessed the matching of oxygen supply to demand in patients using the SD of OEF values across the

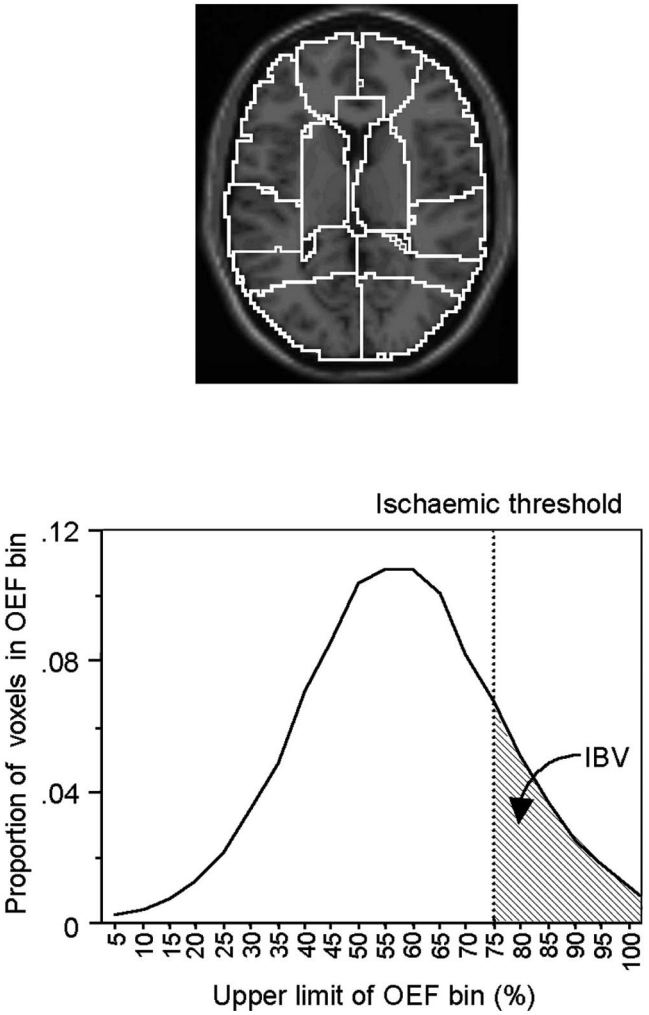

Figure 1. Methodology. *Top*, T1 weighted image of reference brain indicating the 15 regions of interest: right and left medial frontal, lateral frontal, temporal, parietal, occipital, deep gray matter, cerebellum, and the brain stem. *Bottom*, oxygen extraction fraction (*OEF*) histogram from a single patient, showing the distribution of the number of voxels in each OEF bin. Critical OEF thresholds are derived by calculation of the OEF value above which cerebral venous oxygen content would be <3.5 mL/100 mL. The summed volume of voxels above this threshold is the ischemic brain volume (*IBV*).

15 ROIs and by calculation of the SD of the OEF histograms (SD OEF). These variables were compared between volunteers and patient groups. Since focal lesions could provide a simple structural cause for abnormal OEF distributions, we also repeated this comparison after excluding ROIs that showed abnormalities on structural computed tomography images.

Metabolic Effects of Hyperventilation. We have previously published data on test-retest variability in ^{15}O PET studies (29). The acquisition of ^{15}O PET data in two frames in both the baseline and posthyperventilation images provided the opportunity of using individual frames to calculate four independent sets of metabolic images, which could be used to assess reproducibility of $CMRO_2$ measurements specifically within this study population. We used the average SD for the $CMRO_2$ measurements obtained in 18 patients to calculate the population 95% prediction interval (PI) for zero change (using two SD values). We then calculated the number and proportion of ROIs with increases or decreases in $CMRO_2$ greater than these limits. In this way we could define the statistical relevance of changes in $CMRO_2$ following hyperventilation.

Although these average data are extremely useful, the calculated SD could vary within individual patients and within particular ROIs in patients. It would therefore be helpful to have a more specific measure of variability within each individual subject who participated in an interventional study. The acquisition of ^{15}O PET data in two frames provided the opportunity to use these individual frames to assess reproducibility for each ROI in each subject. However, the small sample numbers (two readings both before and after hyperventilation) mean that a conventional threshold of change >2 SD cannot be used to assess the statistical significance of changes in this context. Although any estimate of variance based on two degrees of freedom must be treated with caution, statistical theory suggests that an estimate of 95% PIs of zero change may be provided by a threshold of 4.3 SD, and this margin was used to assess the significance of changes from baseline.

Electrophysiology

SEP data were recorded following median nerve stimulation at the wrist (0.2-msec square wave pulses at 4 Hz). More than 450 sweeps were averaged at ten stimulus intensities presented in a pseudorandom order (10–100 mA, in 10 mA increments), with a bandpass of 3–3000 Hz. Silver/silver chloride disc electrodes (10 mm in diameter) sited 5 cm posterior and 7 cm lateral to the vertex were used to record the primary cortical response (N20–P27). An electrode placed at Fz (International 10:20 convention) was used as the reference. Scalp electrode impedances were maintained <5000 Ω. SEP waveforms were labeled according to the nomenclature of Mauguiere (43).

The SEP data were analyzed by measuring the amplitude of the primary cortical response (N20–P27). This was conducted at each of the stimulus intensities to produce a stimulus response curve for the left and right hemispheres. Two measurements were made from each SEP stimulus response curve: the stimulus intensity required to elicit the half maximal cortical evoked response of the N20–P27 component (ES_{50}) and the maximum N20–P27 amplitude. It was not possible to obtain bilateral measurements in all subjects due to cranial surgery.

Comparison of Electrophysiology and PET Data. We obtained 26 measurements from 14 patients with head injury (Table 1). SEP data were recorded immediately after the corresponding PET session without any change in physiology or treatment variables. Group comparisons of SEP data and $CMRO_2$ were undertaken by correlating the ES_{50} to $CMRO_2$ in an ROI that included the contralateral sensorimotor cortex. All patients with a lesion within the ROI were excluded due to inadequate signal for data processing.

Effects of Hyperventilation. We obtained a further 12 SEP recordings from nine patients to assess the electrophysiologic effects of hyperventilation. Within-subject comparisons of changes in cortical excitability with hyperventilation were quantified by comparing the maximum N20–P27 amplitude obtained at baseline and following intervention.

Statistical Analysis. Statistical analysis was undertaken using Statview (version 5, 1998, SAS Institute, Cary, NC). All data are expressed and displayed as mean ± SD, unless otherwise stated. Global, ROI, and voxel-based PET data were compared using two-tailed paired and unpaired *t*-tests and analysis of variance as appropriate. Following statistical advice, individual ROIs were treated independently after

Bonferroni correction, since they represented a clinically relevant method of segmenting the brain to look for regional ischemia, with specific location being irrelevant to this analysis.

There was considerable variation in the magnitude and direction of changes in PET-derived metabolic variables with hyperventilation. These data were therefore displayed as box and whisker plots and changes were assessed using nonparametric statistics (Wilcoxon's signed-rank test and the Mann-Whitney U Test). The significance of changes in $CMRO_2$ with hyperventilation was assessed by defining the number of ROIs with increases or decreases in $CMRO_2$ greater than the 95% PI for zero change. Linear regression was used to compare changes in PET variables (ΔCBF, $\Delta CMRO_2$, and ΔOEF) and the relationship between ES_{50} and $CMRO_2$. Changes in SEP variables with hyperventilation were assessed using paired *t*-tests. All *p* values are quoted after Bonferroni corrections (where appropriate), and corrected *p* values $<.05$ were considered significant.

RESULTS

Global Physiology

The data for ten control subjects and 18 patients at baseline and following hyperventilation are shown in Table 2. SjO_2 remained >50% in all patients.

Regional Physiology

Hyperventilation led to a significant reduction in CBF and increase in OEF (Fig. 2, $p < .001$, Wilcoxon's signed-rank test with Bonferroni correction). Changes in CBV with hyperventilation were less consistent. There was considerable variability in $CMRO_2$ change, and although some ROIs showed reductions in $CMRO_2$ with hyperventilation, $CMRO_2$ values showed a small but significant overall increase with hyperventilation across the 270 ROIs (Fig. 2, $p < .001$, Wilcoxon's signed-rank test with Bonferroni correction).

Estimation of ischemic burden. Compared with baseline, OEF distributions obtained following hyperventilation were shifted toward higher values (Fig. 3).

Normocapnic patients showed a significantly higher IBV than controls (17 ± 22 vs. 2 ± 3 mL, $p \leq .05$, unpaired *t*-test), which was increased further following hyperventilation (88 ± 66 vs. 17 ± 22 mL, $p < .0001$, paired *t*-test) (Fig. 4).

The maximum IBV was 255 mL (18% of brain volume) following hyperventilation. Although ischemic volumes were a variable proportion of the total brain volume (range 1–18%), these voxels were often in frontal, temporal, and parietal regions, in areas associated with neurocognitive function (Fig. 5).

Perfusion utilization matching. There was no statistically significant relationship between ΔCBF and $\Delta CMRO_2$ (Fig. 6), and there was great variability within individual subjects. Despite this, the data appear to suggest that many regions demonstrate an increase in $CMRO_2$ despite the reduction in CBF but that a decrease in $CMRO_2$ is more likely as CBF is severely reduced.

Correlation of ΔOEF and $\Delta CMRO_2$ showed no statistically significant relationship ($r^2 = .01$, $p = .1$). Within individual subjects this relationship was variable but generally stronger, with a median (range) r^2 value of .3 (−.2 to .92) and median (range) *p* value of .07 (<.0001–.95). However, when independent $^{15}O_2$ and $H_2{}^{15}O$ emission maps were used to calculate $CMRO_2$ and OEF, there was no clear relationship between these variables.

OEF values across the 15 regions in individual subjects showed a significantly wider SD in normocapnic patients than in controls (4.8 ± 1.9 vs. 3 ± 0.6 %, $p < .01$, unpaired *t*-test), suggesting less uniform and efficient matching of oxygen delivery to demand in the patients. These differences were retained when regions that contained structural lesions were excluded ($p < .01$). Following hyperventilation the SD increased (5.6 ± 2.3 vs. 4.8 ± 1.9, $p < .01$, paired *t*-test), implying a further deterioration in flow-metabolism cou-

Table 2. Mean ± SD for $Paco_2$, cerebral perfusion pressure (CPP), intracranial pressure (ICP), jugular venous saturation (SjO_2), global cerebral blood flow (CBF), cerebral blood volume (CBV), cerebral oxygen metabolism ($CMRO_2$), and oxygen extraction fraction (OEF) in ten healthy controls and 18 patients with head injury

Global Data	Control	Normocapnic Patients	Hypocapnic Patients
$Paco_2$, torr	41 ± 3	36 ± 3[a]	29 ± 2[b]
CPP, mm Hg		79 ± 8	84 ± 9
ICP, mm Hg		17 ± 7	15 ± 6
SjO_2, %		69 ± 6	57 ± 5[b]
CBF, mL/100 mL/min	37 ± 5	34 ± 10	27 ± 8[b]
CBV, mL/100 mL	3.7 ± 0.8	4.3 ± 0.5[c]	4.3 ± 0.6
$CMRO_2$, μmol/100 mL/min	123 ± 16	78 ± 16[a]	81 ± 19
OEF, %	43 ± 3	38 ± 7	49 ± 6[b]

[a] $p < .001$, unpaired *t*-test with Bonferroni correction for comparison between normocapnic patients and controls; [b] $p < .001$, paired *t*-test with Bonferroni correction for comparison between normocapnia and hypocapnia; [c] $p < .05$, unpaired *t*-test with Bonferroni correction for comparison between normocapnic patients and controls.

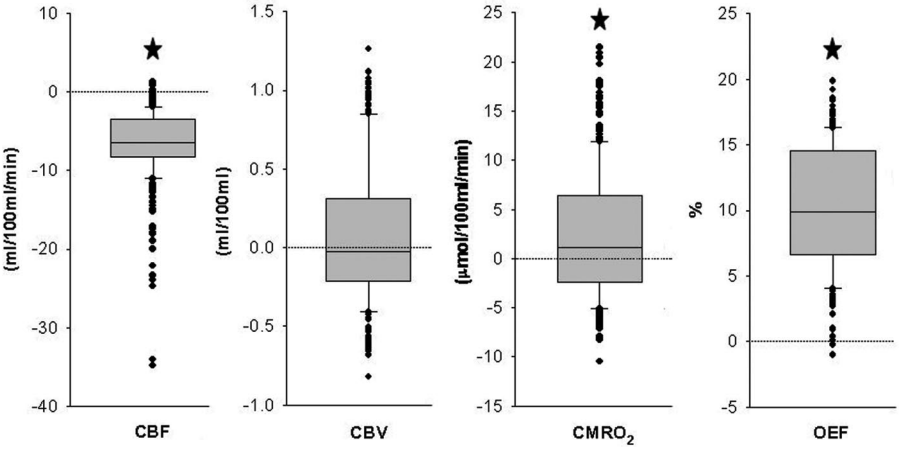

Figure 2. Effect of hyperventilation on regional physiology. Box and whisker plots of changes (Δ) in cerebral blood flow (*CBF*), cerebral blood volume (*CBV*), cerebral oxygen metabolism($CMRO_2$), and oxygen extraction fraction (*OEF*) produced by hyperventilation in 15 regions of interest (ROIs) in 18 subjects between 2 and 7 days postinjury (270 ROIs in total). The central lines in each box denote median values, the lower and upper boundaries the 25th and 75th centile, the error bars the 10th and 90th centile, and the closed circles outlying data points. *$p < .001$, Wilcoxon's signed-rank test with Bonferroni correction, comparing normocapnic and hypocapnic values.

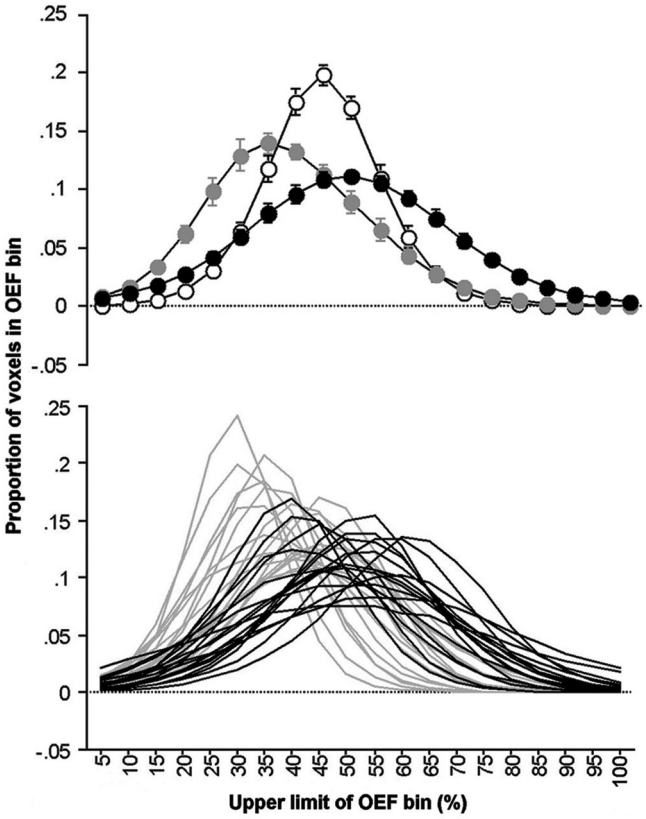

Figure 3. Oxygen extraction fraction (*OEF*) histograms. *Top*, mean ± SE OEF histograms (showing proportion of voxels in each OEF bin) in ten controls (*white*) and in 18 patients following head injury, at relative normocapnia (*gray*; mean $Paco_2$ 36 torr [4.8 kPa]) and after hyperventilation (*black*; mean $Paco_2$ 29 torr [3.9 kPa]). *Bottom*, individual patient OEF histograms at normocapnia (*gray*) and following hyperventilation (*black*). Note the rightward shift of the curves with an increase in the number of voxels with critically high OEF values.

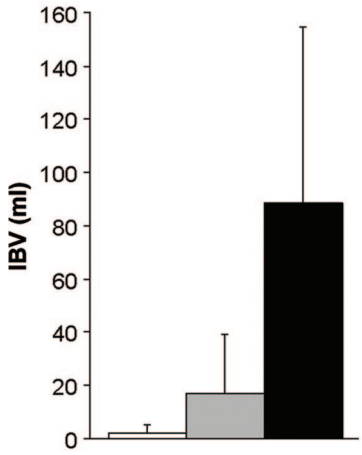

Figure 4. Estimation of ischemic brain volume (*IBV*). Mean + SD ischemic brain volumes in controls (*white*) and in head-injured patients at relative normocapnia (*gray*; mean $Paco_2$ 36 torr [4.8 kPa]) and after hyperventilation (*black*; mean $Paco_2$ 29 torr [3.9 kPa]). *$p < .0001$, paired *t*-test for comparison between normocapnic and hypocapnic values.

pling. In addition, the OEF histograms from patients were broader with regions of high and low OEF (Fig. 3). This is demonstrated by the fact that the SD of the OEF histograms was wider in normocapnic patients compared with controls (15.8 ± 4.1 vs. 10.5 ± 1.5%, $p < .001$ unpaired *t*-test) and increased with hyperventilation (19.8 ± 5 vs. 15.8 ± 4.1%, $p < .0001$ paired *t*-test).

Metabolic Effects of Hyperventilation

Using the measurements of $CMRO_2$ obtained from the two baseline and two posthyperventilation frames, we used analysis of variance to determine the significance of the differences (Table 3).

Although the degree of change will obviously depend on whether the subject is hyperventilated, it is also dependent on both subject and brain region. Although there is a significant interaction between brain region and subject, the lack of a significant three-way interaction suggests that these influences act independently. The residual variance of the $CMRO_2$ measurements that could not be accounted for by the known independent variables was 8.22, and therefore the calculated SD for the $CMRO_2$ measurements was 2.87 μmol/100 mL/min.

Those regions with a change in $CMRO_2$ greater than the population 95% PI for zero change are shown in Figure 6. Twenty-seven percent of ROIs examined showed increases in $CMRO_2$, whereas 7% showed reductions in $CMRO_2$ following hyperventilation. When changes in $CMRO_2$ were compared using the individually calculated 95% PI for zero change (4.3 SD), 23% and 9% of ROIs showed increases and decreases, respectively. When compared with ROIs without structural pathology, ROIs that contained lesions showed no systematic difference in $CMRO_2$ responses following hyperventilation ($p = .73$, Mann-Whitney U test). Reductions in $CMRO_2$ with hyperventilation were not confined to a small minority of patients. Using population and individually calculated thresholds described previously, significant reductions in $CMRO_2$ were observed in one or more ROIs in five (28%) and six (33%) of the 18 patients studied respectively.

Electrophysiology

Cortical excitability measured as the ES_{50} was linearly related to resting regional $CMRO_2$ in 14 patients within an ROI that included the primary somatosensory cortex ($r^2 = -.49$, $p < .001$, Fig. 7). A reduction of $Paco_2$ from 36 ± 3 torr (4.8 ± 0.4 kPa) to 29 ± 2 torr (3.8 ± 0.3 kPa) in nine patients led to a significant increase in the maximum SEP N20–P27 amplitude obtained (2.3 ± 0.9 vs. 1.8 ± 0.9 μV, $p < .001$, paired *t*-test).

DISCUSSION

We have combined ^{15}O PET and measurement of cerebral electrophysiology to examine the effects of acute hyperventilation following TBI. We have shown that the acute decrease in CBF caused by hyperventilation leads to a significant increase in the volume of brain at risk of ischemia and deterioration in flow-metabolism coupling. The metabolic response to hyperventilation was extremely variable, and although some regions demonstrated a significant decrease in $CMRO_2$, overall it was slightly increased. Cerebral electrophysiology was signifi-

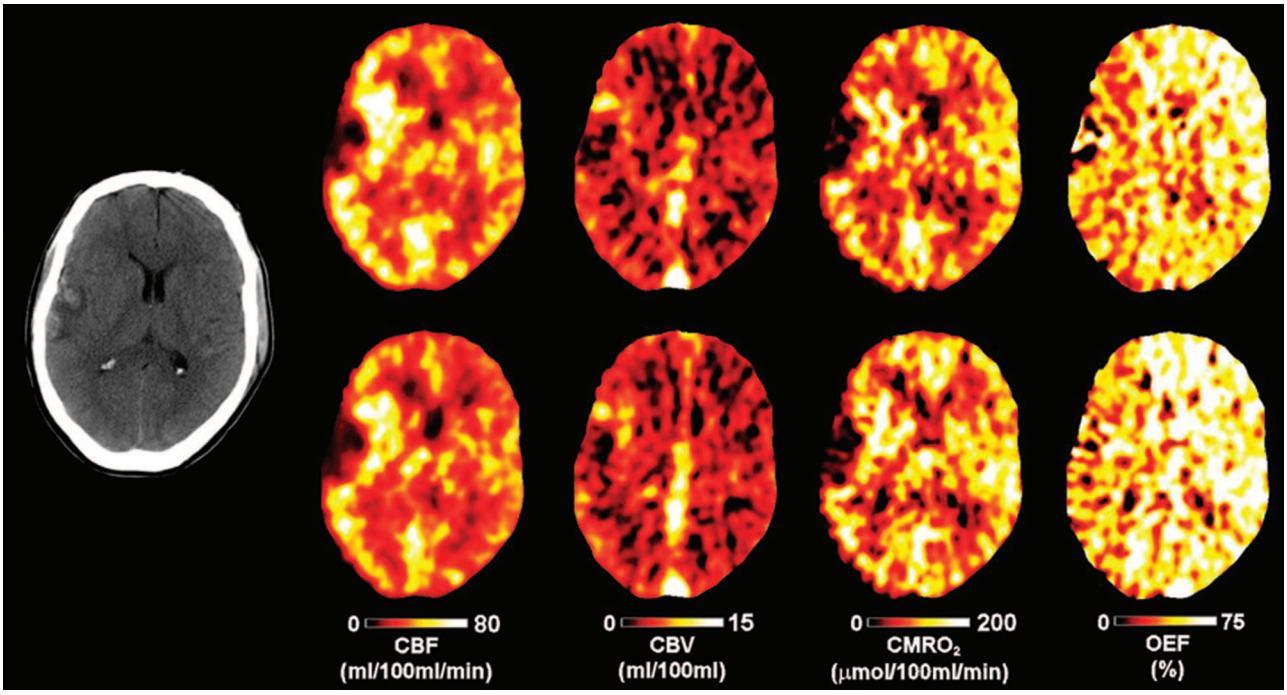

Figure 5. Positron emission tomography (PET) images following acute hyperventilation. Radiograph computed tomography, PET cerebral blood flow (*CBF*), cerebral blood volume (*CBV*), cerebral oxygen metabolism ($CMRO_2$), and oxygen extraction fraction (*OEF*) images obtained from a 45-yr-old male 3 days after head injury at relative normocapnia (*top panel*, $Paco_2$ 35 torr [4.7 kPa]) and hypocapnia (*bottom panel*, $Paco_2$ 29 torr [3.8 kPa]). Note the right temporoparietal hemorrhagic contusion. Baseline intracranial pressure (ICP) 22 mm Hg, cerebral perfusion pressure (CPP) 73 mm Hg, and jugular venous saturation (SjO_2) 70% were consistent with hyperemia and support the use of hyperventilation for ICP control. Hyperventilation reduced ICP to 17 mm Hg and increased CPP to 80 mm Hg, with a reduction of SjO_2 to 54%. Despite these relative improvements, baseline ischemic brain volume was 44 mL and increased to 135 mL with hyperventilation. These increases were observed in both perilesional and normal regions of brain tissue.

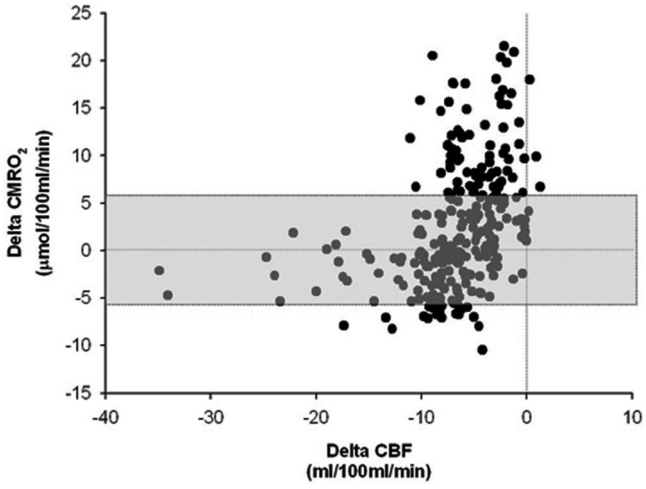

Figure 6. Relationship between Δ cerebral blood flow (*CBF*) and Δ cerebral oxygen metabolism ($CMRO_2$) with hyperventilation. Scattergram of the relationship between ΔCBF and ΔCMRO2 in 270 regions of interest from 18 patients. The horizontal shaded boxes represent the population 95% prediction interval for zero change in repeated measurements for cerebral metabolism.

cantly correlated with baseline $CMRO_2$, and in a subset of patients, we found that hyperventilation led to a significant increase in the amplitude of the cortical SEP response. These data suggest that the known effects of hyperventilation on neuronal excitability (44–46) are associated with an increase in $CMRO_2$ in head-injured patients. The increase in $CMRO_2$ despite a reduction in CBF necessitates a substantial increase in OEF, which may result in neuronal injury. Indeed, some brain regions showed a significant decrease in $CMRO_2$ following the hyperventilation challenge. This study provides further evidence of the potential harm of hyperventilation therapy in some regions of the injured brain.

Defining Ischemia in Head Injury

Conventional functional imaging approaches in clinical and experimental stroke have traditionally used CBF thresholds for ischemia and have succeeded in identifying useful predictive values for tissue survival or death (19–21). However, the situation in head injury is confounded by the use of sedative agents and by the metabolic effects of trauma (23, 24), which may cause primary reductions in cerebral metabolism; coupled CBF decreases in this context would not represent ischemia. Under these circumstances the only true measure of the adequacy of CBF is a measurement of the OEF. We provide data on ischemic brain volumes using a calculated threshold OEF value that, if sustained for a period of time, may result in neuronal damage (37, 38). The imbalance in flow-metabolism coupling denoted by high OEF values characterizes tissue at

Table 3. Analysis of variance table for the cerebral oxygen metabolism measurements for the four ^{15}O positron emission tomography frames obtained from 15 regions within 18 subjects

	df	Sum of Squares	Mean Square	F Value	*p* Value
Brain region	14	80,936.9	5781.2	702.950	<.0001
Subject	17	290,582.4	17,093.1	2078.385	<.0001
Hyperventilation	1	2064.8	2064.8	251.060	<.0001
Region/subject	238	51,200.4	215.1	26.158	<.0001
Region/hyperventilation	14	245.3	17.5	2.130	.0094
Subject/hyperventilation	17	12,827.9	754.6	91.751	<.0001
Region/subject/hyperventilation	238	1813.8	7.6	0.927	.7499
Residual	540	4441.1	8.2		

df, degrees of freedom.

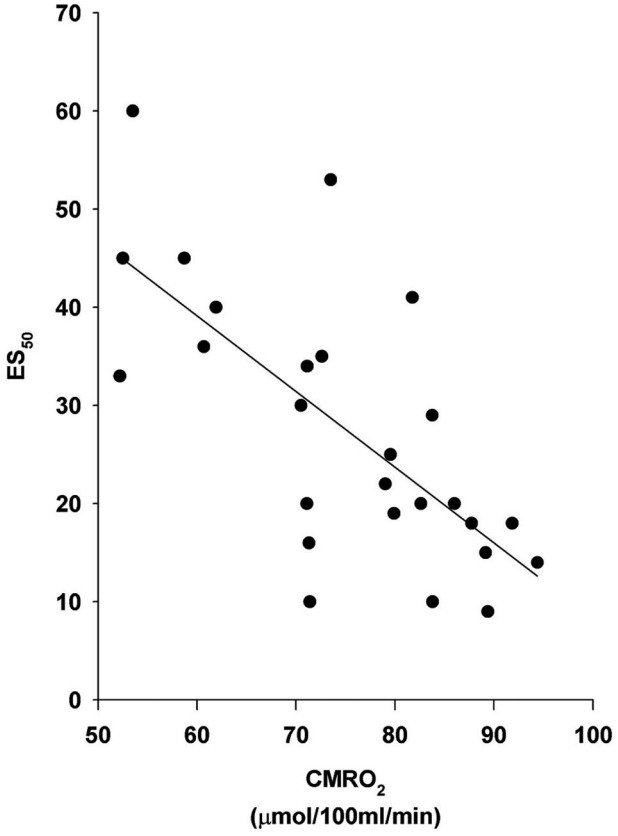

Figure 7. Relationship between cerebral oxygen metabolism (*$CMRO_2$*) and half maximal cortical evoked response of the N20–P27 component (*ES_{50}*). Linear regression plot of ES_{50} vs. $CMRO_2$ in a parietal region of interest including the primary somatosensory cortex. The graph is based on 26 data sets obtained at normocapnia from 14 patients with head injury ($r^2 = -.49$, $p < .001$).

high risk of ischemic injury. The OEF threshold that we use is based on the best available data and is clinically relevant in terms of the management of head injury, where we wish to prevent the occurrence of further neuronal injury.

Close matching of flow to metabolism normally results in remarkably little variation in OEF across the brain despite wide regional variations in CBF and $CMRO_2$ (42). The wider based OEF histograms following hyperventilation suggest that matching of perfusion to oxygen utilization is impaired (Fig. 3). Although lower emission statistics could produce more extreme OEF values in the setting of reduced blood flow in such voxel-based measurements, the ROI-based estimate of OEF spread is much less susceptible to noise and provides independent quantitative confirmation of our findings. Importantly, the increase in the SD of the OEF distribution is not purely related to an increase in OEF, since there remains a significant volume of tissue with low OEF suggestive of hyperemia. The coexistence of relative ischemia and hyperemia following hyperventilation in some patients may represent a more fundamental problem with matching of perfusion to oxygen utilization following head injury.

The use of voxel-based analysis to define tissue at risk is new in this context but has been used in other settings such as stroke (47). However, statistics in such voxel-based measurements are less robust than those from larger ROIs, and the calculated spread of values in metabolic maps may increase when emission counts are reduced, as with low CBF values in head-injured patients. The concern is that this would result in more extreme values, which might translate into more voxels with high OEF values and broader OEF distributions. We have examined this issue in experiments using brain phantoms and control clinical data (37). Although it is clear that a reduction in emission statistics as a consequence of low blood flow will lead to an increase in the measured IBV and SD of the OEF distribution, these methodological effects do not account for the large IBV values that we observe following hyperventilation.

Effect of Hyperventilation on Cerebral Metabolism

Tissue with "misery perfusion" is traditionally defined as having reduced CBF, high OEF, and maintained $CMRO_2$ (18). If such compromise is sustained, perfusion is reduced further, and/or metabolic demand increases, neuronal death will occur (18). Although global CBF measurements (3) and CBF imaging techniques (9, 10, 12) have shown that hyperventilation produces significant reductions in perfusion, it is impossible to establish the significance of these changes without sequential measurements of OEF and $CMRO_2$ before and after hyperventilation. One previous PET study of hyperventilation found no evidence of global ischemia with moderate reductions in $Paco_2$ (14). It is unlikely, however, that such global measurements would detect regional ischemia. A more recent study from the same group (15) used an ROI-based analysis but showed no reduction in mean $CMRO_2$, even in regions with posthyperventilation CBF values as low as 10 mL/100 mL/min. These results suggest that hyperventilation does not uniformly produce acute ischemia and neuronal injury despite a decrease in CBF and increase in OEF. However, this conclusion is based on data averaging across all ROIs and

cannot exclude the possibility that critical ischemia and neuronal injury may result in a significant subpopulation of ROIs, especially when the response to hyperventilation is heterogeneous (12). Furthermore, it would seem inappropriate to use perfusion thresholds to select ROIs for analysis, when increased OEF levels and the inability to maintain $CMRO_2$ should be used to define ischemia and neuronal injury respectively.

Although we found no change in global $CMRO_2$ with hyperventilation, we found that $CMRO_2$ was increased overall within the 15 ROIs in all patients. This implies that hyperventilation, at least initially, does not result in neuronal injury and in fact may increase $CMRO_2$. However, we wished to investigate whether acute hyperventilation could result in a decrease in $CMRO_2$ within some regions of the injured brain. Although the majority of brain regions showed either no change (66%) or an increase (27%) in $CMRO_2$, 7% of the ROIs studied showed reductions in $CMRO_2$ that exceeded the 95% prediction limits. We considered that these results could have been affected by variations in SD measurements within individuals, which could have resulted in $CMRO_2$ changes being incorrectly classified as significant. In fact, when recalculated using a calculated 95% PI for zero change based on 4.3 individual SD values, the results were comparable. These data suggest that acute hyperventilation not only reduces CBF but may do so to an extent that compromises oxidative metabolism in some regions of the injured brain. Indeed, the CBF reductions with hyperventilation resulted in $CMRO_2$ reductions in at least one ROI in 28% of patients, despite increases in OEF.

Although those regions that showed a decrease in $CMRO_2$ tended to suffer the greatest reductions in CBF, this relationship was not statistically significant. Examination of the relationship between ΔOEF and $\Delta CMRO_2$ within individual subjects suggested that those regions showing a reduction in $CMRO_2$ tended to show the smallest increase in OEF following hyperventilation. However, this relationship was lost following exclusion of shared variables within the calculated PET variables (29, 48). Although this may have been related to the lower signal to noise characteristics of the independent emission frames used, it is difficult to draw firm conclusions from these data.

The finding of increased $CMRO_2$ overall requires some explanation. Changes in arterial CO_2 partial pressures have powerful effects on brain function (44–46). In particular, hyperventilation can induce seizures (45) and enhance neuronal excitability (44, 46). Our SEP data are in keeping with previous studies that demonstrate increases in cortical SEP amplitudes in humans with hypocapnia (49) and changes in cerebral glucose consumption (50, 51) with experimentally induced changes in cerebral pH. We demonstrate that cortical excitability measured by the ES_{50} correlates with regional $CMRO_2$. In addition, we show that the SEP N20–P27 amplitude is increased following hyperventilation in head-injured patients. Conventionally, ischemia is associated with a reduction in cortical SEP amplitude (52), and an increase in SEP amplitudes would not appear to be consistent with ischemia. Although our data are clearly not suggestive of global ischemia, they imply that the global physiologic changes induced by hyperventilation may predispose to regional ischemia and neuronal damage in some patients following head injury. The increased oxygen demand in the face of reduced oxygen delivery represents a particularly severe physiologic insult to the injured brain. Brain regions where neuronal activity increased, measured as an increase in SEP cortical amplitudes, were only able to maintain (or increase) $CMRO_2$ through increases in OEF, and some ROIs were unable to maintain $CMRO_2$ despite increases in OEF.

We aimed to identify evidence of misery perfusion using critically increased OEF values (based on a cerebral venous oxygen content <3.5 mL/100 mL) (37, 38) and evidence of neuronal injury by examining regions with a reduction in $CMRO_2$. We identified a significant increase in the volume of brain at potential risk of ischemic damage and found that some brain regions studied showed a decrease in $CMRO_2$ following hyperventilation. However, even if $CMRO_2$ is maintained acutely, it is unsafe to assume that brain regions with OEF values far in excess of the normal range (48, 53) would be able to sustain such increases. Decompensation could occur over time or be precipitated by physiologic insults such as fever or fits (which increase oxygen demand) or transient reductions in blood pressure (which decrease oxygen delivery). The evidence is that these insults occur in $>90\%$ of severely head injured patients in well-run intensive care units (54). Although this study does not demonstrate that hyperventilation results in cerebral infarction or poor outcome, the resulting changes in cerebral physiology are of concern. Indeed, we have previously shown that patients who demonstrate early increases in IBV are more likely to suffer poor outcome (38). Clearly, assessment of the hazards of hyperventilation will need more studies, with longer term follow-up data to resolve these issues fully. However, we need to take account of these risks when considering the clinical implications of our data and their interpretation. As always in medicine, we should first ensure that we do no harm.

Ethical considerations meant that we were unable to take patients with marked elevations in intracranial pressure for PET studies. Although such patients would clearly benefit from a reduction in intracranial pressure, we have little data to quantify the effects of acute hyperventilation on ICP, CBF, and $CMRO_2$ in this setting. Only four of our patients had a baseline ICP >20 mm Hg and only one >25 mm Hg. Consequently, we are unable to address whether the relative risks and benefits of hyperventilation might be different in the presence of marked intracranial hypertension. However, there was no systematic effect of baseline ICP on change in $CMRO_2$ ($r^2 = .044$, $p = .69$).

CONCLUSIONS

We show that levels of hypocapnia that are deemed permissible by authoritative guidelines (2) may result in significant regional ischemia within 10 days of head injury. This is significant because conventional wisdom accepts a role for modest hyperventilation during this "hyperemic" phase of head injury (2, 55). Throughout all study protocols SjO_2 values remained $>50\%$, a widely accepted threshold (2) for defining cerebral ischemia. The failure of common bedside monitors to detect such regional ischemia means that we can no longer rely on these conventional SjO_2 thresholds to provide protection against ischemia. As a consequence, "acceptable" hyperventilation may cause harm that remains clinically undetected.

ACKNOWLEDGMENTS

We thank Dr. J. C. Matthews and the members of the Wolfson Brain Imaging Centre for all their help in conducting these studies.

REFERENCES

1. Madden JA: The effect of carbon dioxide on cerebral arteries. *Pharmacol Ther* 1993; 59: 229–250
2. The Brain Trauma Foundation. The American Association of Neurological Surgeons. The Joint Section on Neurotrauma and Critical Care. *J Neurotrauma* 2000; 17:457–627
3. Yundt KD, Diringer MN: The use of hyperventilation and its impact on cerebral ischemia in the treatment of traumatic brain injury. *Crit Care Clin* 1997; 13:163–184
4. Marion DW, Firlik A, McLaughlin MR: Hyperventilation therapy for severe traumatic brain injury. *New Horiz* 1995; 3:439–447
5. Bouma GJ, Muizelaar JP, Choi SC, et al: Cerebral circulation and metabolism after severe traumatic brain injury: The elusive role of ischemia. *J Neurosurg* 1991; 75:685–693
6. Bouma GJ, Muizelaar JP, Stringer WA, et al: Ultra-early evaluation of regional cerebral blood flow in severely head-injured patients using xenon-enhanced computerized tomography. *J Neurosurg* 1992; 77:360–368
7. Marion DW, Darby J, Yonas H: Acute regional cerebral blood flow changes caused by severe head injuries. *J Neurosurg* 1991; 74:407–414
8. Obrist WD, Langfitt TW, Jaggi JL, et al: Cerebral blood flow and metabolism in comatose patients with acute head injury. Relationship to intracranial hypertension. *J Neurosurg* 1984; 61:241–253
9. McLaughlin MR, Marion DW: Cerebral blood flow and vasoresponsivity within and around cerebral contusions. *J Neurosurg* 1996; 85: 871–876
10. Skippen P, Seear M, Poskitt K, et al: Effect of hyperventilation on regional cerebral blood flow in head-injured children. *Crit Care Med* 1997; 25:1402–1409
11. Stringer WA, Hasso AN, Thompson JR, et al: Hyperventilation-induced cerebral ischemia in patients with acute brain lesions: Demonstration by xenon-enhanced CT. *AJNR Am J Neuroradiol* 1993; 14:475–484
12. Coles JP, Minhas PS, Fryer TD, et al: Effect of hyperventilation on cerebral blood flow in traumatic head injury: clinical relevance and monitoring correlates. *Crit Care Med* 2002; 30:1950–1959
13. Muizelaar JP, Marmarou A, Ward JD, et al: Adverse effects of prolonged hyperventilation in patients with severe head injury: A randomized clinical trial. *J Neurosurg* 1991; 75: 731–739
14. Diringer MN, Yundt K, Videen TO, et al: No reduction in cerebral metabolism as a result of early moderate hyperventilation following severe traumatic brain injury. *J Neurosurg* 2000; 92:7–13
15. Diringer MN, Videen TO, Yundt K, et al: Regional cerebrovascular and metabolic effects of hyperventilation after severe traumatic brain injury. *J Neurosurg* 2002; 96: 103–108
16. Stocchetti N, Maas AI, Chieregato A, et al: Hyperventilation in head injury: A review. *Chest* 2005; 127:1812–1827
17. Astrup J, Siesjo BK, Symon L: Thresholds in cerebral ischemia—The ischemic penumbra. *Stroke* 1981; 12:723–725
18. Baron J: Mapping the ischaemic penumbra with PET: Implications for acute stroke treatment. *Cerebrovasc Dis* 1999; 9:193–201
19. Powers WJ, Grubb RL Jr, Darriet D, et al: Cerebral blood flow and cerebral metabolic rate of oxygen requirements for cerebral function and viability in humans. *J Cereb Blood Flow Metab* 1985; 5:600–608
20. Marchal G, Beaudouin V, Rioux P, et al: Prolonged persistence of substantial volumes of potentially viable brain tissue after stroke: A correlative PET-CT study with voxel-based data analysis. *Stroke* 1996; 27:599–606
21. Heiss WD, Huber M, Fink GR, et al: Progressive derangement of periinfarct viable tissue in ischemic stroke. *J Cereb Blood Flow Metab* 1992; 12:193–203
22. Cunningham AS, Salvador R, Coles JP, et al: Physiological thresholds for irreversible tissue damage in contusional regions following traumatic brain injury. *Brain* 2005; 128: 1931–1942
23. Verweij BH, Muizelaar JP, Vinas FC, et al: Impaired cerebral mitochondrial function after traumatic brain injury in humans. *J Neurosurg* 2000; 93:815–820
24. Bergsneider M, Hovda DA, Lee SM, et al: Dissociation of cerebral glucose metabolism and level of consciousness during the period of metabolic depression following human traumatic brain injury. *J Neurotrauma* 2000; 17:389–401
25. Jennett B, Bond M: Assessment of outcome after severe brain damage. A practical scale. *Lancet* 1975; 1:480–484
26. Marshall LF, Marshall SB, Klauber MR, et al: A new classification of head injury based on computerized tomography. *J Neurosurg* 1991; 75:S14–S27
27. Teasdale G, Jennett B: Assessment of coma and impaired consciousness. A practical scale. *Lancet* 1974; 2:81–84
28. Menon DK: Cerebral protection in severe brain injury: Physiological determinants of outcome and their optimisation. *Br Med Bull* 1999; 55:226–258
29. Coles JP, Fryer TD, Bradley PG, et al: Intersubject variability and reproducibility of 15O PET studies. *J Cereb Blood Flow Metab* 2006; 26:48–57
30. Smielewski P, Coles JP, Fryer TD, et al: Integrated image analysis solutions for pet datasets in damaged brain. *J Clin Monit Comput* 2002; 17:427–440
31. Studholme C, Hill DL, Hawkes DJ: Automated 3-D registration of MR and CT images of the head. *Med Image Anal* 1996; 1:163–175
32. Studholme C, Hill DL, Hawkes DJ: Automated three-dimensional registration of magnetic resonance and positron emission tomography brain images by multiresolution optimization of voxel similarity measures. *Med Phys* 1997; 24:25–35
33. Talairach J, Tournoux P: Co-planar Stereotaxic Atlas of the Human Brain. Stuttgart, Thieme, 1998
34. Correia JA, Alpert NM, Buxton RB, et al: Analysis of some errors in the measurement of oxygen extraction and oxygen consumption by the equilibrium inhalation method. *J Cereb Blood Flow Metab* 1985; 5:591–599
35. Baron JC, Frackowiak RS, Herholz K, et al: Use of PET methods for measurement of cerebral energy metabolism and hemodynamics in cerebrovascular disease. *J Cereb Blood Flow Metab* 1989; 9:723–742
36. Herscovitch P, Raichle ME: Effect of tissue heterogeneity on the measurement of cerebral blood flow with the equilibrium C15O2 inhalation technique. *J Cereb Blood Flow Metab* 1983; 3:407–415
37. Coles JP, Fryer TD, Smielewski P, et al: Defining ischemic burden after traumatic brain injury using 15O PET imaging of cerebral physiology. *J Cereb Blood Flow Metab* 2004; 24:191–201
38. Coles JP, Fryer TD, Smielewski P, et al: Incidence and mechanisms of cerebral ischemia in early clinical head injury. *J Cereb Blood Flow Metab* 2004; 24:202–211
39. Gibbs EL, Lennox WG, Nims LF, et al: Arterial and cerebral venous blood: Arterial-Venous differences in man. *J Biol Chem* 1942; 144:325–332
40. Robertson CS, Cormio M: Cerebral metabolic management. *New Horiz* 1995; 3:410–422
41. Kety SS, Schmidt CF: The nitrous oxide method for the quantitative determination of cerebral blood flow in man: Theory, procedure and normal values. *J Clin Invest* 1948; 27:476–483
42. Lebrun-Grandie P, Baron JC, Soussaline F, et al: Coupling between regional blood flow and oxygen utilization in the normal human brain. A study with positron tomography and oxygen 15. *Arch Neurol* 1983; 40:230–236
43. Mauguiere F: Somatosensory evoked potentials; normal responses, abnormal waveforms and clinical applications in neurological diseases. *In:* Electrocephalography: Basic Principles, Clinical Applications and Related fields. Niedermeyer E, Lopes Da Silva F (Eds). Baltimore, Williams and Wilkins, 1999, pp 1014–1058
44. Balestrino M, Somjen GG: Concentration of carbon dioxide, interstitial pH and synaptic transmission in hippocampal formation of the rat. *J Physiol* 1988; 396:247–266
45. Lee J, Taira T, Pihlaja P, et al: Effects of CO2 on excitatory transmission apparently caused by changes in intracellular pH in the rat hippocampal slice. *Brain Res* 1996; 706:210–216
46. Huttunen J, Tolvanen H, Heinonen E, et al: Effects of voluntary hyperventilation on cortical sensory responses. Electroencephalographic and magnetoencephalographic studies. *Exp Brain Res* 1999; 125:248–254

47. Marchal G, Benali K, Iglesias S, et al: Voxel-based mapping of irreversible ischaemic damage with PET in acute stroke. *Brain* 1999; 122:2387–2400
48. Frackowiak RS, Lenzi GL, Jones T, et al: Quantitative measurement of regional cerebral blood flow and oxygen metabolism in man using 15O and positron emission tomography: Theory, procedure, and normal values. *J Comput Assist Tomogr* 1980; 4:727–736
49. Ledsome JR, Cole C, Sharp-Kehl JM: Somatosensory evoked potentials during hypoxia and hypocapnia in conscious humans. *Can J Anaesth* 1996; 43:1025–1029
50. Van Nimmen D, Weyne J, Demeester G, et al: Local cerebral glucose utilization in systemic acidosis. *Am J Physiol* 1984; 247: R639–R645
51. Van Nimmen D, Weyne J, Demeester G, et al: Local cerebral glucose utilization during intracerebral pH changes. *J Cereb Blood Flow Metab* 1986; 6:584–589
52. Branston NM, Ladds A, Symon L, et al: Comparison of the effects of ischaemia on early components of the somatosensory evoked potential in brainstem, thalamus, and cerebral cortex. *J Cereb Blood Flow Metab* 1984; 4:68–81
53. Leenders KL, Perani D, Lammertsma AA, et al: Cerebral blood flow, blood volume and oxygen utilization. Normal values and effect of age. *Brain* 1990; 113:27–47
54. Jones PA, Andrews PJ, Midgley S, et al: Measuring the burden of secondary insults in head-injured patients during intensive care. *J Neurosurg Anesthesiol* 1994;6: 4–14
55. Martin NA, Patwardhan RV, Alexander MJ, et al: Characterization of cerebral hemodynamic phases following severe head trauma: Hypoperfusion, hyperemia, and vasospasm. *J Neurosurg* 1997; 87:9–19